AGU ADVANCING EARTH AND SPACE SCIENCES

Geophysical Research Letters

RESEARCH LETTER
10.1029/2025GL118643

Antarctic Meltwater-Stratification Feedback Is Less Pronounced Under High Climate Forcing

Moritz Kreuzer[1,2], Torsten Albrecht[1,3], Willem Huiskamp[1], Stefan Petri[1], Johannes Feldmann[1], Georg Feulner[1,2], and Ricarda Winkelmann[1,2,3]

[1]Potsdam Institute for Climate Impact Research (PIK), Member of the Leibniz Association, Potsdam, Germany, [2]University of Potsdam, Institute of Physics and Astronomy, Potsdam, Germany, [3]Department of Integrative Earth System Science, Max Planck Institute of Geoanthropology, Jena, Germany

Key Points:

- Sub-surface ocean temperature increase due to additional Antarctic meltwater input weakens under strong climate warming
- Climate warming weakens vertical overturning in the Southern Ocean, making the additional effect of meltwater input less significant
- Both warming and additional Antarctic meltwater independently increase ocean stratification, but their combined impact is non-additive

Supporting Information:

Supporting Information may be found in the online version of this article.

Correspondence to:

M. Kreuzer,
kreuzer@pik-potsdam.de

Citation:

Kreuzer, M., Albrecht, T., Huiskamp, W., Petri, S., Feldmann, J., Feulner, G., & Winkelmann, R. (2026). Antarctic meltwater-stratification feedback is less pronounced under high climate forcing. *Geophysical Research Letters*, *53*, e2025GL118643. https://doi.org/10.1029/2025GL118643

Received 8 AUG 2025
Accepted 24 MAR 2026

Author Contributions:

Conceptualization: Moritz Kreuzer, Torsten Albrecht, Georg Feulner, Ricarda Winkelmann
Data curation: Moritz Kreuzer
Formal analysis: Moritz Kreuzer
Funding acquisition: Moritz Kreuzer, Torsten Albrecht, Ricarda Winkelmann
Investigation: Moritz Kreuzer
Methodology: Moritz Kreuzer, Willem Huiskamp, Stefan Petri, Georg Feulner, Ricarda Winkelmann
Software: Moritz Kreuzer, Torsten Albrecht, Stefan Petri
Supervision: Torsten Albrecht, Willem Huiskamp, Stefan Petri,

Abstract Several studies have shown sub-surface warming in the Southern Ocean via an increase in meltwater flux from the Antarctic Ice Sheet (AIS), which can lead to a positive feedback through enhanced basal melting. In this study, we investigate how the feedback strength is related to the prevailing climate in a coupled climate–ice-sheet model. We find that sub-surface temperature increase due to Antarctic meltwater is more pronounced under pre-industrial climate compared to a strong global warming scenario. This is explained by a climate-change induced reduction of vertical overturning in the Southern Ocean, which already leads to strong sub-surface warming without additional meltwater. While in the pre-industrial climate additional meltwater substantially reduces vertical mixing, the additional ice-sheet mass flux into the ocean has less impact when the overturning is already suppressed by climate change. Sub-surface warming due to meltwater flux increase thereby shows a saturation effect under climate warming.

Plain Language Summary The melting of the Antarctic Ice Sheet increases with global warming and computer experiments have shown a resulting increase of surrounding ocean temperatures below the surface. As the warmer waters come into contact with the Antarctic ice mass, even more melting can occur, potentially resulting in a self-amplifying feedback loop. Using computer simulations, this study shows that the feedback strength is dependent on the climate system state. In a warmer climate, where ocean temperatures are higher, the effect of meltwater on temperature below the ocean surface is smaller compared to no climate change. Understanding the mechanisms of climate and ice-sheet interactions is important to correctly project future changes of sea level and climate warming. The methods used in this study are an example of how computer models can be advanced to more realistically represent these complex interactions.

1. Introduction

The Antarctic Ice Sheet (AIS) has been losing mass for several decades (Otosaka et al., 2023) and ice loss is projected to accelerate with future warming (Coulon et al., 2024; Seroussi et al., 2020). Higher atmospheric and oceanic temperatures lead to more melting at the ice-sheet surface and below the floating ice shelves, resulting in thinning and acceleration of glacier flow (The IMBIE team, 2018). Several feedback mechanisms influence the ice-sheet's response to a change in forcing, on different temporal and spatial scales (Fyke et al., 2018). These feedbacks can be stabilizing (negative feedback sign), when an initial perturbation is dampened by other processes, such as an initial reduction in ice-sheet height being compensated for by increased snowfall due to higher atmospheric temperatures at lower altitudes (Nicola et al., 2023). On the other hand, feedbacks can also be destabilizing (positive feedback sign), when an initial perturbation is amplified. An example is the Marine Ice Sheet Instability, where an initial grounding line retreat leads to further ice loss on a retrograde slope due to higher ice fluxes in deeper regions (Feldmann & Levermann, 2015; Schoof, 2007).

In addition, ice-sheet changes can have a major impact on the climate system. Increased meltwater, for example, modifies the stratification of the Southern Ocean and local sea-ice dynamics with potentially global climatic implications such as the redistribution of heat and precipitation across the northern and southern hemispheres or an increase in temperature variability (Bronselaer et al., 2018; Golledge et al., 2019). Similarly, large-scale ice-sheet geometry changes influence atmospheric circulation and precipitation patterns (Tewari et al., 2021). Changes in Antarctic surface albedo have also been shown to significantly influence both regional energy balance and global climate dynamics (Booth et al., 2024; Goldner et al., 2014). In order to capture these feedback dynamics, climate and ice-sheet changes must be simulated interactively in coupled models rather than in isolation,

Johannes Feldmann, Georg Feulner, Ricarda Winkelmann
Visualization: Moritz Kreuzer
Writing – original draft: Moritz Kreuzer
Writing – review & editing: Moritz Kreuzer, Torsten Albrecht, Willem Huiskamp, Stefan Petri, Johannes Feldmann, Georg Feulner

as has been common so far (e.g., the latest climate model intercomparison project CMIP6 (Eyring et al., 2016) and the companion initiative for ice sheets ISMIP6 (Nowicki et al., 2016)).

Meltwater from the AIS introduces fresh and therefore light water masses into the Southern Ocean near the freezing point through different mechanisms. Ice-sheet surface runoff reaches the ocean in liquid form either near the surface or via subglacial channels at the grounding line. Melting in ice-shelf cavities and from calved icebergs releases freshwater several hundred meters deep and requires latent heat, which further cools adjacent water masses. This buoyant, cold meltwater accumulates primarily in the top 200 m of the water column, enhancing stratification in the Southern Ocean, which is characterized by a sharp contrast between fresh, cold surface waters and warmer, saltier waters below (see Figures S1 and S2 in Supporting Information S1 in Kreuzer et al., 2025). Strong prevailing westerlies drive northward Ekman transport, resulting in a steepening and shoaling of isopycnals associated with Circumpolar Deep Water south of the Polar Front. This water mixes with the surface via strong mesoscale eddy activity and breaking internal waves (Rintoul, 2018). However, stronger stratification through increased meltwater input inhibits this exchange, leading to a warming of sub-surface waters at intermediate depth and cooling at the surface (Silvano et al., 2018). This change in temperature structure can accelerate basal melting of ice shelves, releasing more meltwater and further intensifying stratification, potentially initiating a self-reinforcing feedback loop (Bronselaer et al., 2018). In the following, we refer to this mechanism as the *meltwater-stratification feedback* (MSF), which is illustrated in Figure S1 in Supporting Information S1.

Sub-surface warming with increased Antarctic freshwater input into the Southern Ocean has been found in several model studies. Fogwill et al. (2015), Stouffer et al. (2007) and Chen et al. (2023), for example, conduct idealized Antarctic meltwater hosing under present-day climate conditions, while others add static (time-invariant) hosing under historic or future climate warming scenarios (e.g., Park & Latif, 2019; Pauling et al., 2016). Some studies also add projected Antarctic melt trajectories in a transient manner to standalone climate models with future warming scenarios (e.g., Bronselaer et al., 2018; Sadai et al., 2020; Schmidt et al., 2023; Thomas et al., 2023). Only a few studies exist that incorporate interactive ice sheets, for example Swingedouw et al. (2008) or D. Li et al. (2024). Golledge et al. (2019) use an iterative "ping-pong" coupling approach between climate and ice-sheet models by repeating the individual component simulation in alternating order for the whole simulation time span. Lambert et al. (2025) quantify the MSF by using linear response functions in order to include this feedback in standalone ice-sheet projections of sea-level rise.

The dependence of the MSF strength on the prevailing climate remains unclear, however. Fogwill et al. (2015) observe sub-surface warming by adding meltwater in a pre-industrial climate and propose that additional climate forcing would further amplify the feedback. On the other hand, Bronselaer et al. (2018) hypothesize that meltwater hosing has less impact under global warming, as the vertical convection would decrease under climate forcing alone. So far, a direct analysis of the MSF strength in dependence of the climate system state is still missing. Furthermore, due to computational limitations imposed by model resolution, most studies focus on interactions over periods of decades or centuries. The time scales of ice-sheet dynamics, however, are multi-centennial or longer.

In this study, we use an interactive climate–ice-sheet model setup to investigate the differences in MSF strength between different climate states on multi-centennial time scales. We define a metric for the feedback quantification and apply it for pre-industrial climate conditions and for a strong climate warming scenario.

2. Models and Experiment Design

For our experiments, we use the coarse-resolution climate model CM2Mc (Galbraith et al., 2011), which has a nominal resolution of 3° and consists of ocean, sea ice, atmosphere and land components. To represent dynamic ice-ocean feedbacks due to additional Antarctic meltwater, we couple CM2Mc to the Parallel Ice Sheet Model (PISM) (Bueler & Brown, 2009; Winkelmann et al., 2011), which allows an interactive modeling of Antarctic land ice. CM2Mc and PISM are coupled via the framework described in Kreuzer et al. (2021) that exchanges fluxes and boundary conditions between the climate and ice-sheet components every 10 years. The framework makes use of the basal melt parameterization PICO (Reese et al., 2018), which parametrizes the vertical overturning circulation in Antarctic ice-shelf cavities based on far-field temperature and salinity input, and is therefore well suited for the coupling between the coarse, non-cavity resolving ocean model with the ice-sheet model.

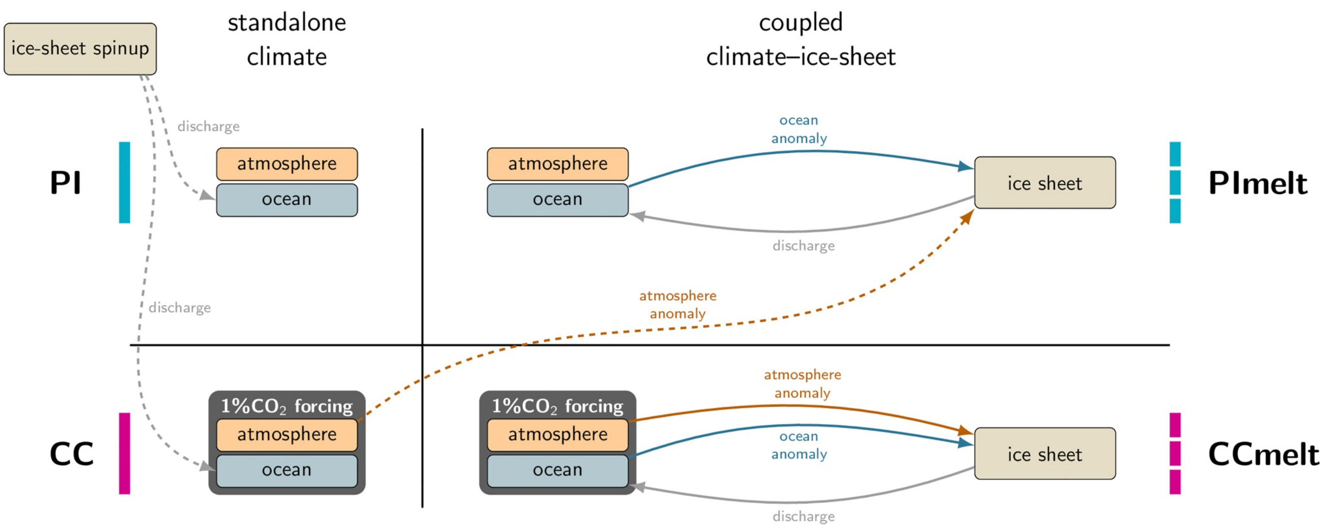

Figure 1. Experiment Design. The study features *standalone climate* model experiments (PI and CC) and *coupled climate–ice-sheet* simulations (PImelt and CCmelt). Dashed arrows indicate non-interactive forcing, for example statically prescribed Antarctic discharge fluxes to PI and CC runs from the ice-sheet spinup simulation. The exchanged variables in coupled climate–ice-sheet simulations are updated every 10 years, which is indicated by solid arrows. The ice-sheet component in CCmelt is interactively forced by both, ocean and atmosphere, components from the climate model. The ice-sheet component in PImelt receives pre-computed (non-interactive) atmospheric forcing from CC (dashed arrow) and dynamically evolving ocean boundary conditions from PImelt ocean component. Atmospheric and oceanic forcing applied to the ice-sheet model is implemented via an anomaly approach as explained in Section 2.

We perform model experiments in two different climate states. One resembles a pre-industrial climate (PI) and the other represents a strong climate change scenario (CC) with an exponential 1 % CO_2 increase during the first 140 years and constant greenhouse gas concentrations thereafter, which is four times the pre-industrial CO_2 concentration. The latter part is run for 600 years, so the simulations cover 740 years in total. During the CC experiment the global mean surface temperature increases by ca. +3°C after 140 years, which is comparable to SSP3-7.0 scenario in 2100, and by ca. +5°C by the end of the simulation, which is more than the best estimate for SSP5-8.5 (+4.4°C) in 2100 (IPCC, 2021) (Figure S2a in Supporting Information S1).

PI and CC are standalone climate model runs featuring a fixed AIS, as Antarctic meltwater fluxes are prescribed statically to the climate model (see Section S2.1 in Supporting Information S1). In the context of this study, we refer to experiments without interactive ice-sheets as "standalone climate" simulations (PI and CC). In the coupled setup, PISM is forced with climate model derived atmospheric and oceanic boundary conditions and provides the corresponding meltwater fluxes back to CM2Mc. These "coupled climate–ice-sheet" experiments are called PImelt and CCmelt, which employ the greenhouse gas concentrations from PI and CC, respectively.

Figure 1 provides an overview of the different experiments. In the coupled climate–ice-sheet experiments PImelt and CCmelt, climatic fields are not applied directly to the ice-sheet due to biases in the climate model. Instead, oceanic and atmospheric anomalies with respect to the climate spinup are provided as forcing to the ice-sheet model, where these anomalies are added to the respective spinup baseline forcing (see Section S1.3 in Supporting Information S1 for more details).

To compare the MSF between the two climate states, a similar Antarctic meltwater perturbation is required. We achieve this by applying comparable atmospheric forcing to PImelt and CCmelt ice-sheets. While the atmospheric anomalies of temperature and precipitation in CCmelt are derived from the coupled climate model, the forcing of the PImelt ice-sheet component is implemented via prescribed (non-interactive) anomalies from CC instead of the PI climate state. The ice-ocean dynamics are fully interactive between PISM and CM2Mc in PImelt, similar to CCmelt (see Figure 1).

A detailed description of both models, the coupling framework, model spinup, as well as a climate control run comparison with observational and reanalysis data is provided in Supporting Information S1.

10.1029/2025GL118643

3. Results

3.1. Meltwater-Stratification Feedback Strength

The increase in ocean temperature at depth due to additional meltwater from the AIS is much more pronounced under pre-industrial climate conditions (PImelt vs. PI) compared with the climate change scenario (CCmelt vs. CC). Figures 2a and 2b show these meltwater-induced ocean temperature differences in zonal mean transects for both climate states, averaged over the last 200 years of simulation. While in PImelt the positive temperature differences reach all the way down to the ocean floor at 5,000 m with maximum values above 1°C, the maximum warming in CCmelt is restricted to ca. 0.2°C and is only present in the upper 2,000 m close to the AIS margin. The depth at which temperature anomalies are retrieved for the ice-sheet model forcing (which we refer to as sub-surface ocean temperature in the following) depends on the local continental shelf bathymetry (see Section S1.3 in Supporting Information S1), and is between 500 and 750 m. While this Antarctic sub-surface temperature (T_i) is about 2°C higher at the end of CC compared to PI, the additional meltwater adds 0.55°C in PImelt compared to 0.26°C in CCmelt, as shown in Figure 2c.

The total amount of additional freshwater inserted into the ocean is comparable between PImelt and CCmelt (ca. +0.04 Sv in year 540–740; $1\ \mathrm{Sv} = 10^6\ \mathrm{kg\,m^{-3}}$; Figure 2d), which is an increase of 44 % compared to PI. The change in ice-sheet discharge (ΔQ_d) is the sum of basal melting, iceberg calving and surface runoff increase with respect to the ice-sheet control state. The ice-sheet component in PImelt receives the effects of warming due to greenhouse gas increase only via the atmospheric boundary and not via the ocean interface as in CCmelt (see Figure 1), which is reflected in a different distribution between the discharge modes. While surface runoff dominates the discharge increase in PImelt, increased mass loss through basal melt and a subsequent reduction in calving characterizes the CCmelt simulation. Detailed information on ice-sheet changes including regional variations and discharge mechanism is provided in Section S2 in Supporting Information S1.

To quantify the strength of the MSF, we divide the sub-surface temperature difference by the corresponding change in meltwater input as

$$\gamma_{ms} = \frac{\Delta T_i}{\Delta Q_d} \qquad (1)$$

The spatially aggregated MSF strength γ_{ms} shows a self-amplyfing behavior between AIS discharge and sub-surface ocean temperatures after ca. 200 years into the simulation for both experiments. The feedback in PImelt is about twice as large as in CCmelt for the last 350 years of simulation (see Figure 2e). The feedback strength is regionally dominated by the Weddell, Ross and East Antarctic regions, which are the biggest contributors to the change in ice-sheet discharge ΔQ_d. Only in the Amundsen region, the feedback is slightly larger in CCmelt scenario compared to PImelt (Section S3 and Figure S9 in Supporting Information S1).

3.2. Vertical Mixing Reduction by Climate and Meltwater Forcing

Inserting additional meltwater under pre-industrial conditions (PImelt vs. PI) reduces vertical mixing of surface and deeper waters in the Southern Ocean drastically. This is shown in maps of Southern Ocean maximum mixed layer depths (Figures 3a and 3b), where the previous main convection site in the Weddell Sea, with mixing depths down to 3,000 m, shuts down almost completely when meltwater increases in PImelt. Antarctic Bottom Water formation (AABW; Figure 3e) reduces from about 19 Sv in PI to 13 Sv in PImelt after year 300 and sea ice expands in the Southern Ocean (Figures 3b and 3f) while the atmosphere cools (Figure S1b in Supporting Information S1). Simultaneously, the AMOC strength increases by a few Sv in PImelt (Figure S1c in Supporting Information S1), which could be explained by the inter-hemispheric seesaw effect (Willeit et al., 2025). Vertical profiles in the Weddell Sea show a strong salinity decline, most prominent at the surface (Figure 3g), where most additional meltwater is inserted, resulting in a steeper density gradient (Figure 3i) and increased buoyancy frequency (Figure 3j). The reduction in vertical mixing leads to warming below 200 m and cooling above (Figure 3h).

The greenhouse gas forcing in CC results in strong surface warming (Figures S2a and S2b in Supporting Information S1), which reduces AABW (Figure 3e) and AMOC (Figure S2c in Supporting Information S1) compared to PI through globally enhanced stratification. The subsequent strong reduction in sea-ice extent

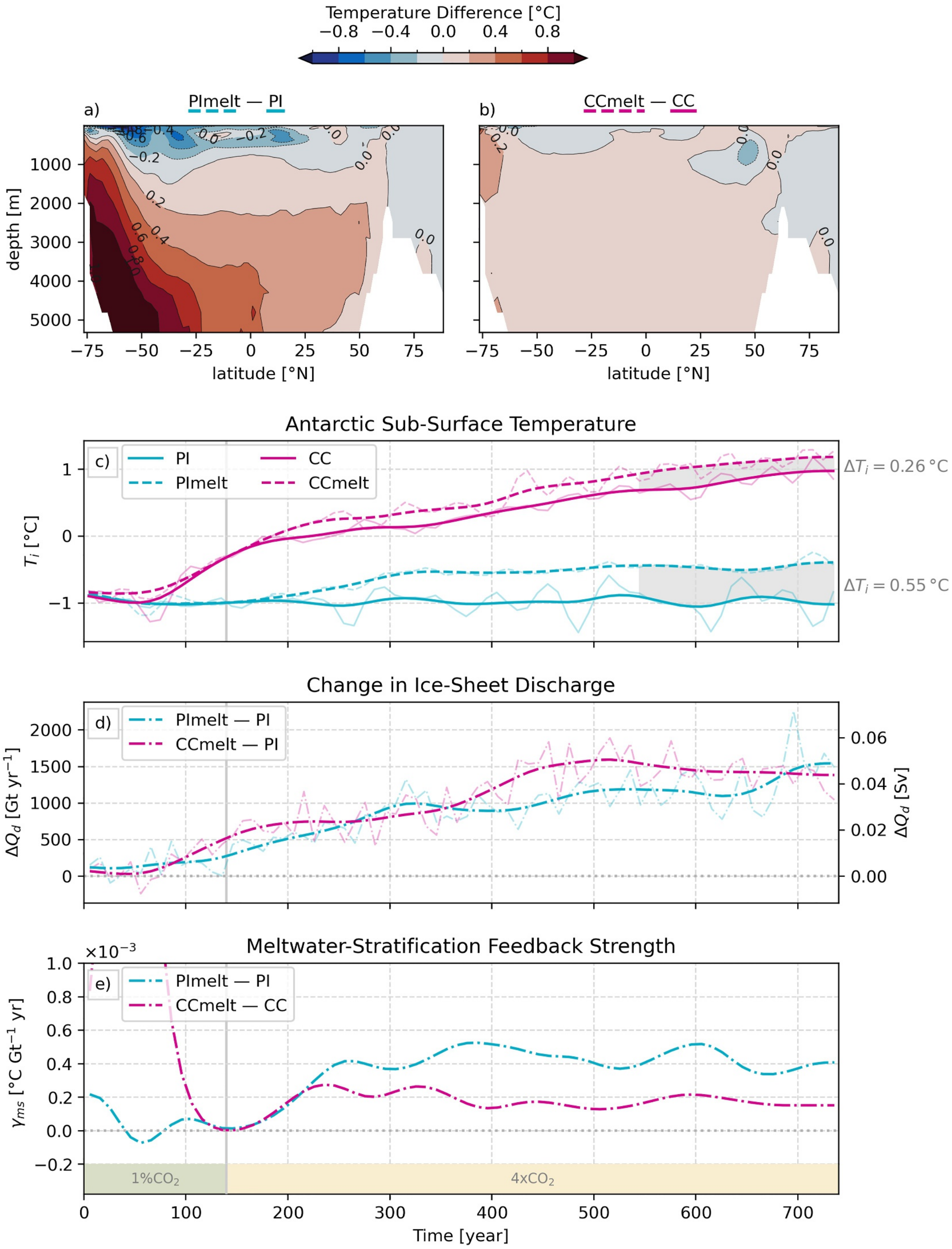

Figure 2. Sub-surface ocean warming and meltwater-stratification feedback (MSF) strength. Transect of zonal mean temperature difference for (a) PImelt – PI and (b) CCmelt – CC averaged over the time period 540–740. Figure S5 in Supporting Information S1 shows reference profiles for PI, CC and their difference. (c) Time evolution of sub-surface ocean temperature T_i (PISM-PICO input averaged over all ice-sheet basins). Gray areas in the last 200 years show the time-averaged, meltwater-induced anomaly ΔT_i. (d) Change in ice-sheet discharge ΔQ_d with respect to a PI control simulation (see Section S2.1 in Supporting Information S1 for more information, also about partitioning of the meltwater flux into different modes). (e) MSF strength γ_{ms}. Time series show butterworth lowpass filtered signal (cutoff frequency: 150 years) in the foreground and decadal data with lighter colors in the background in (c) and (d). Meltwater strength γ_{ms} (e) is calculated from lowpass filtered signals of (c) and (d).

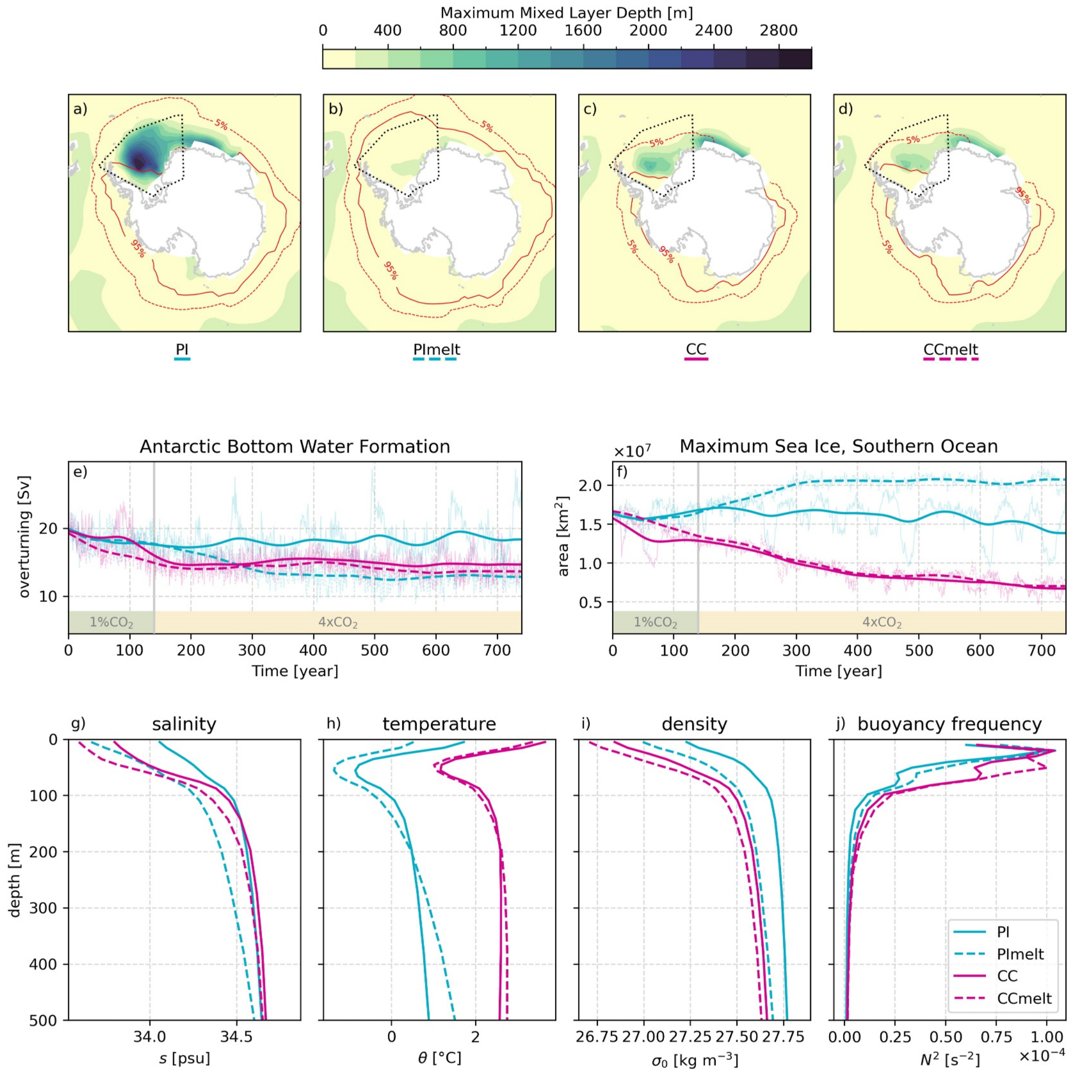

Figure 3. Vertical mixing changes in Southern Ocean. (a–d) Maximum mixed layer depth for the different experiments averaged over the time period 540–740. Maximum sea-ice extent is shown with red contour lines, where 95% temporal coverage between 540 and 740 (all seasons) is marked with solid, and 5% temporal coverage is marked with dashed lines. (e) AABW time series, which is the maximum annual mean of the overturning stream function between 90°S and 0°S and below 2,000 m. (f) Time series of maximum sea-ice extent in the Southern Hemisphere. Time series (e) and (f) show butterworth lowpass filtered signal (cutoff frequency: 150 years) in the foreground and yearly data with lighter colors in the background. Vertical profiles of practical salinity (g), potential temperature (f), potential density (i) and buoyancy frequency (j) as year 540–740 mean and horizontally averaged over the Weddell Sea region marked by dashed lines in panels (a–d).

(Figures 3c and 3f) leads to reduced salinity in the upper 100 m (Figure 3g) through less brine rejection from sea-ice formation. In combination with the effect of temperature increase on density (Figure 3h), the water column in CC is stronger stratified compared to PImelt (Figure 3i), which is also reflected in a higher buoyancy frequency (Figure 3j). However, CC facilitates stronger AABW (Figure 3e) and deeper mixed layer depth (Figures 3b and 3c) due to the strongly reduced maximum sea-ice extent (solid red contours in Figures 3a–3c), allowing open ocean convection despite a stronger stratified water column.

Adding additional meltwater to CC causes a further reduction in surface salinity (Figure 3g) leading to increased stratification (Figure 3i) and buoyancy frequency (Figure 3j) in CCmelt. Similar to the pre-industrial control case, the additional meltwater leads to an increase in sea-ice cover (Figures 3d and 3f) accompanied by surface air temperature cooling (Figure S2b in Supporting Information S1), reduction in mixed layer depth (Figure 3d) and AABW (Figure 3e). However, the effect is much smaller compared to PI versus PImelt, as sea-ice extent is strongly suppressed by climate forcing in CCmelt, which results in a smaller effect on the vertical ocean temperature structure with cooling at the surface and warming at depth (Figure 3h).

4. Discussion

Using the coarse grid, cavity-parameterized CM2Mc-PISM coupling framework, sub-surface ocean warming occurs with additional ice-sheet meltwater input on a circum-Antarctic scale. As higher temperature forcing generates more basal melt, this results in a self-amplifying feedback with respect to ice-sheet mass loss. This is in line with previous meltwater hosing studies like Fogwill et al. (2015) or Bronselaer et al. (2018). However, our study shows that the feedback strength reduces under a strong climate forcing scenario (CC) compared to the addition of meltwater in the PI control simulation by ca. 50 %. Our methodology uses a new model approach, that interactively couples a global climate and an Antarctic ice-sheet model in order to represent the ice-ocean feedback of additional melting due to increased sub-surface ocean temperature. Previous studies have prescribed additional meltwater in a non-interactive manner (e.g., Thomas et al., 2023) or make use of an iterative "ping-pong" coupling (Golledge et al., 2019) to account for ice-ocean feedback in multiple steps.

Notably, hosing experiments with higher horizontal resolution (≤1°) find a spatially heterogeneous pattern in the continental shelf temperatures with increased Antarctic meltwater input, namely a sub-surface cooling in the Bellingshausen and Amundsen Sea and a warming in other regions (e.g., Beadling et al., 2022; Moorman et al., 2020; Muilwijk et al., 2026). Those studies find sub-surface warming to be linked to stronger stratification of the water column, which reduces the formation of Dense Shelf Water and thereby also upward vertical heat transport. The localized sub-surface cooling, on the other hand, arises from a speed up of the Antarctic Slope Current (ASC), which is driven by the lateral density gradient between the continental shelf and the open ocean. A stronger ASC shields the shelf from intrusions of warm Circumpolar Deep Water, while at the same time traps added coastal freshwater through reduced cross-shelf exchange. In addition, less dense shelf waters in the Weddell Sea, which are too buoyant to descend into the ocean abyss, are transported westward around the Antarctic Peninsula into the Bellingshausen and Amundsen Seas (Beadling et al., 2022; Moorman et al., 2020; Muilwijk et al., 2026). While eddy-resolving models (e.g., 0.1° resolution) enable a realistic ASC representation, they limit model experiments to several decades due to the high computational costs (Ong et al., 2025).

Our CM2Mc model with a nominal resolution of 3° resolution is too coarse to realistically represent the continental shelf bathymetry, nor does it resolve fine-scale dynamics like the ASC, which explains the differences in spatial response. Importantly, it also forms Antarctic Bottom Water through open-ocean convection rather than through Dense Shelf Water production on the continental shelf and subsequent export into the abyssal ocean, which is a common issue among low-resolution models (Heuzé, 2021). Nevertheless, the qualitative response of sub-surface ocean warming and reduced vertical mixing due to increased Antarctic meltwater input is the same between models that realistically represent continental shelf processes (Q. Li et al., 2023) and the coarser models (Bronselaer et al., 2018; Chen et al., 2023). Whether our findings of reduced MSF under climate change are robust remains to be verified with higher-resolution models.

Some global climate models are able to simulate ice-shelf cavities and resolve the ocean dynamics within them (e.g., Comeau et al., 2022; Siahaan et al., 2022; Song et al., 2025), which improves local ocean dynamics compared to closed cavities (Hutchinson et al., 2023), but is not common yet. We make use of the sub-shelf cavity module PICO to parameterize the overturning circulation within the ice-shelf cavities. While all basal melt-rate parameterizations introduce biases (Burgard et al., 2022), PICO has been shown to simulate mean basal melt rates within observed ranges (Reese et al., 2018) and with a quadratic melt sensitivity to ocean temperatures as in a cavity-resolving ocean model (Reese et al., 2023). We insert the resulting freshwater fluxes from basal melt at depth of the calving front into the water column. While this is in principle more realistic than an insertion at surface, Mathiot et al. (2017) demonstrated that a meltwater distribution between the grounding line and the calving front depth is necessary in order to simulate the resulting overturning circulation correctly. Even in a 1° model inserting basal melt throughout the water column can lead to sub-surface cooling similar to higher resolution models (e.g., Moorman et al., 2020), instead of a sub-surface warming when adding basal melt at surface (Thomas et al., 2023). In our configuration, the insertion depth is relatively shallow, generally ranging from 50 to 200 m, depending on the ice-sheet state and basin. This limits the influence of shifts in meltwater modes, between surface runoff, basal melting, and calving, such as those occurring between the PImelt and CCmelt experiments (see Section S2.1 in Supporting Information S1). While surface runoff decreases slightly in CCmelt compared to

PImelt, the biggest change is an increase in basal melt and a reduction in calving, both extracting latent heat from the ocean.

Similar to many CMIP6 models, CM2Mc exhibits significant positive temperature biases at the Antarctic continental margin, which are up to +2°C compared to reanalysis data (Figure S4c in Supporting Information S1) (Heuzé, 2021; Muilwijk et al., 2026). Due to this bias, we do not feed the modeled ocean properties directly into PISM-PICO, but use an anomaly approach instead. The baseline forcing is observational data at the continental shelf floor averaged over the period 1975–2012 (Schmidtko et al., 2014). Changes in modeled sub-surface ocean temperature and salinity are then added to the baseline forcing and subsequently provided as input to the basal melt parameterization PICO. For atmospheric forcing of surface air temperature and precipitation, we follow a similar approach (Section S1.3 in Supporting Information S1). A simplification in our modeling approach is also the insertion of iceberg calving fluxes at the coastal margin instead of a distributed input over a wider area in the Southern Ocean and at depth, which would be more realistic (Hoffman et al., 2024). Ackermann et al. (2024) find a reduction of vertical stratification and a subsequent increase of deep-water formation as a result of realistic representation of iceberg trajectories.

CM2Mc shows internal variability and quasi-periodic behavior of open-ocean deep convection (Cabré et al., 2017). For simplicity, we focus on the multi-decadal model mean results in this study. We provide more information about the quasi-oscillatory occurrence of deep convection in the Section S4 in Supporting Information S1 and also discuss a model drift of the PI control run after the year 740.

5. Conclusion

With an interactively coupled climate–ice-sheet model framework, this study investigates the MSF with respect to the prevailing climate on multi-centennial time scales. Climate warming strengthens vertical stratification in the Southern Ocean, which reduces the destabilizing effect of additional Antarctic meltwater compared to a scenario without climate change. Thereby, the resulting sub-surface warming effect due to ice-sheet discharge decreases with climate warming. While the coarse model resolution enables a feedback analysis on multi-centennial time scales with a dynamically evolving ice-sheet response, the representation of small-scale dynamic features like the ASC is missing. Therefore, future work remains with higher resolution and cavity-resolving coupled models to test the robustness of these results.

Conflict of Interest

The authors declare no conflicts of interest relevant to this study.

Availability Statement

The modified code of CM2Mc climate model used in this study is preserved at Zenodo (record 17360862) via Kreuzer (2025a), licensed under GNU General Public License v2.0 and developed openly at https://github.com/mom-ocean/MOM5. The modified code of PISM ice-sheet model used in this study is preserved at Zenodo (record 16642252) via Khrulev et al. (2025), licensed under GNU General Public License v3.0 and developed openly at https://github.com/pism/pism. The coupling framework code used to couple CM2Mc and PISM in this study is preserved at Zenodo (record 16643820) via Kreuzer (2025b), licensed under GNU General Public License v3.0 and developed openly at https://github.com/m-kreuzer/PISM-MOM_coupling/. The model output data used in the study are available at Zenodo (record 18713398) via Kreuzer (2026) with CC BY 4.0 license.

Acknowledgments
The authors gratefully acknowledge the European Regional Development Fund (ERDF), the German Federal Ministry of Education and Research, and the state of Brandenburg for supporting this project by providing resources for the high-performance computer system at the Potsdam Institute for Climate Impact Research (PIK). This research was supported by Ocean Cryosphere Exchanges in ANtarctica: Impacts on Climate and the Earth system, OCEAN ICE, which is funded by the European Union, Horizon Europe Funding Programme for research and innovation under Grant agreement Nr. 101060452, 10.3030/101060452. OCEAN ICE contribution number 32. This work was supported by the Deutsche Forschungsgemeinschaft (DFG) in the framework of the priority program SPP 1158 "Antarctic Research with comparative investigations in Arctic ice areas" by the following grants: WI 4556/4-1, WI 4556/6-1. Moritz Kreuzer was financially supported by the Potsdam Graduate School. Willem Huiskamp is part of PIK's Planetary Boundaries Science Lab and is funded by Virgin Unite. The work of Torsten Albrecht and Ricarda Winkelmann has been conducted within the framework of the PalMod project (Grant FKZ: 01LP1925D, 01LP1918B, 01LP2305B), supported by the German Federal Ministry of Education and Research (BMBF) as a Research for Sustainability initiative (FONA). Development of PISM is supported by NASA Grant 20-CRYO2020-0052 and 80NSSC22K0274 and NSF Grant OAC-2118285. The authors thank Pedro Colombo for discussions about the basal melt input at depth implementation in MOM5, Julius Garbe for providing the initial PISM ice-sheet setup and Birte Gülk for proof-reading the manuscript. Open Access funding enabled and organized by Projekt DEAL.

References

Ackermann, L., Rackow, T., Himstedt, K., Gierz, P., Knorr, G., & Lohmann, G. (2024). A comprehensive Earth system model (AWI-ESM2.1) with interactive icebergs: Effects on surface and deep-ocean characteristics. *Geoscientific Model Development*, *17*(8), 3279–3301. https://doi.org/10.5194/gmd-17-3279-2024

Beadling, R. L., Krasting, J. P., Griffies, S. M., Hurlin, W. J., Bronselaer, B., Russell, J. L., et al. (2022). Importance of the antarctic slope current in the Southern Ocean response to ice sheet melt and wind stress change. *Journal of Geophysical Research: Oceans*, *127*(5), e2021JC017608. https://doi.org/10.1029/2021JC017608

Booth, A., Goodwin, P., & Cael, B. B. (2024). Ice sheet-albedo feedback estimated from Most recent deglaciation. *Geophysical Research Letters*, *51*(15), e2024GL109953. https://doi.org/10.1029/2024GL109953

Bronselaer, B., Winton, M., Griffies, S. M., Hurlin, W. J., Rodgers, K. B., Sergienko, O. V., et al. (2018). Change in future climate due to Antarctic meltwater. *Nature*, *564*(7734), 53–58. https://doi.org/10.1038/s41586-018-0712-z

Bueler, E., & Brown, J. (2009). Shallow shelf approximation as a "sliding law" in a thermomechanically coupled ice sheet model. *Journal of Geophysical Research*, *114*(F3), F03008. https://doi.org/10.1029/2008JF001179

Burgard, C., Jourdain, N. C., Reese, R., Jenkins, A., & Mathiot, P. (2022). An assessment of basal melt parameterisations for antarctic ice shelves. *The Cryosphere*, *16*(12), 4931–4975. https://doi.org/10.5194/tc-16-4931-2022

Cabré, A., Marinov, I., & Gnanadesikan, A. (2017). Global atmospheric teleconnections and multidecadal climate oscillations driven by Southern Ocean convection. *Journal of Climate*, *30*(20), 8107–8126. https://doi.org/10.1175/JCLI-D-16-0741.1

Chen, J.-J., Swart, N. C., Beadling, R., Cheng, X., Hattermann, T., Jüling, A., et al. (2023). Reduced deep convection and bottom water formation due to antarctic meltwater in a multi-model ensemble. *Geophysical Research Letters*, *50*(24), e2023GL106492. https://doi.org/10.1029/2023GL106492

Comeau, D., Asay-Davis, X. S., Begeman, C. B., Hoffman, M. J., Lin, W., Petersen, M. R., et al. (2022). The DOE E3SM v1.2 cryosphere configuration: Description and simulated antarctic ice-shelf basal melting. *Journal of Advances in Modeling Earth Systems*, *14*(2), e2021MS002468. https://doi.org/10.1029/2021MS002468

Coulon, V., Klose, A. K., Kittel, C., Edwards, T., Turner, F., Winkelmann, R., & Pattyn, F. (2024). Disentangling the drivers of future antarctic ice loss with a historically calibrated ice-sheet model. *The Cryosphere*, *18*(2), 653–681. https://doi.org/10.5194/tc-18-653-2024

Eyring, V., Bony, S., Meehl, G. A., Senior, C. A., Stevens, B., Stouffer, R. J., & Taylor, K. E. (2016). Overview of the coupled model intercomparison project phase 6 (CMIP6) experimental design and organization. *Geoscientific Model Development*, *9*(5), 1937–1958. https://doi.org/10.5194/gmd-9-1937-2016

Feldmann, J., & Levermann, A. (2015). Collapse of the west Antarctic ice sheet after local destabilization of the Amundsen basin. *Proceedings of the National Academy of Sciences*, *112*(46), 14191–14196. https://doi.org/10.1073/pnas.1512482112

Fogwill, C. J., Phipps, S. J., Turney, C. S. M., & Golledge, N. R. (2015). Sensitivity of the Southern Ocean to enhanced regional Antarctic ice sheet meltwater input. *Earth's Future*, *3*(10), 317–329. https://doi.org/10.1002/2015EF000306

Fyke, J., Sergienko, O., Löfverström, M., Price, S., & Lenaerts, J. T. M. (2018). An overview of interactions and feedbacks between ice sheets and the Earth system. *Reviews of Geophysics*, *56*(2), 361–408. https://doi.org/10.1029/2018RG000600

Galbraith, E. D., Kwon, E. Y., Gnanadesikan, A., Rodgers, K. B., Griffies, S. M., Bianchi, D., et al. (2011). Climate variability and radiocarbon in the CM2Mc Earth system model. *Journal of Climate*, *24*(16), 4230–4254. https://doi.org/10.1175/2011JCLI3919.1

Goldner, A., Herold, N., & Huber, M. (2014). Antarctic glaciation caused ocean circulation changes at the Eocene–Oligocene transition. *Nature*, *511*(7511), 574–577. https://doi.org/10.1038/nature13597

Golledge, N. R., Keller, E. D., Gomez, N., Naughten, K. A., Bernales, J., Trusel, L. D., & Edwards, T. L. (2019). Global environmental consequences of twenty-first-century ice-sheet melt. *Nature*, *566*(7742), 65–72. https://doi.org/10.1038/s41586-019-0889-9

Heuzé, C. (2021). Antarctic bottom water and north Atlantic deep water in CMIP6 models. *Ocean Science*, *17*(1), 59–90. https://doi.org/10.5194/os-17-59-2021

Hoffman, M. J., Branecky Begeman, C., Asay-Davis, X. S., Comeau, D., Barthel, A., Price, S. F., & Wolfe, J. D. (2024). Ice-shelf freshwater triggers for the Filchner–Ronne ice shelf melt tipping point in a global ocean–sea-ice model. *The Cryosphere*, *18*(6), 2917–2937. https://doi.org/10.5194/tc-18-2917-2024

Hutchinson, K., Deshayes, J., Éthé, C., Rousset, C., de Lavergne, C., Vancoppenolle, M., et al. (2023). Improving Antarctic bottom water precursors in NEMO for climate applications. *Geoscientific Model Development*, *16*(12), 3629–3650. https://doi.org/10.5194/gmd-16-3629-2023

IPCC. (2021). Summary for policymakers [Book Section]. In V. Masson-Delmotte, P. Zhai, A. Pirani, S. L. Connors, C. Péan, S. Berger, et al. (Eds.), *Climate change 2021: The physical science basis. Contribution of working group I to the sixth assessment report of the intergovernmental panel on climate change* (pp. 1–31). Cambridge University Press. https://doi.org/10.1017/9781009157896.001

Khrulev, C., Bueler, E., Aschwanden, A., damaxwell, Brown, J., Albrecht, T., et al. (2025). m-kreuzer/pism: Version as used in paper "Antarctic meltwater-stratification feedbackis less pronounced under high climate forcing" [Software]. *Zenodo*. https://doi.org/10.5281/zenodo.16642252

Kreuzer, M. (2025a). CM2Mc code as used in paper "Antarctic meltwater-stratification feedback is less pronounced under high climate forcing" [Software]. *Zenodo*. https://doi.org/10.5281/zenodo.17360862

Kreuzer, M. (2025b). m-kreuzer/PISM-MOM_coupling: Version as used in paper "Antarctic meltwater-stratification feedback is less pronounced under high climate forcing" [Software]. *Zenodo*. https://doi.org/10.5281/zenodo.16643820

Kreuzer, M. (2026). Data publication for paper "Antarctic meltwater-stratification feedback is less pronounced under high climate forcing". *Zenodo*. https://doi.org/10.5281/zenodo.18713398

Kreuzer, M., Albrecht, T., Nicola, L., Reese, R., & Winkelmann, R. (2025). Bathymetry-constrained impact of relative sea-level change on basal melting in Antarctica. *The Cryosphere*, *19*(3), 1181–1203. https://doi.org/10.5194/tc-19-1181-2025

Kreuzer, M., Reese, R., Huiskamp, W. N., Petri, S., Albrecht, T., Feulner, G., & Winkelmann, R. (2021). Coupling framework (1.0) for the PISM (1.1.4) ice sheet model and the MOM5 (5.1.0) ocean model via the PICO ice shelf cavity model in an antarctic domain. *Geoscientific Model Development*, *14*(6), 3697–3714. https://doi.org/10.5194/gmd-14-3697-2021

Lambert, E., Le Bars, D., Van der Linden, E., Jüling, A., & Drijfhout, S. (2025). Quantifying the feedback between antarctic meltwater release and subsurface Southern Ocean warming. *Earth System Dynamics*, *16*(4), 1303–1323. https://doi.org/10.5194/esd-16-1303-2025

Li, D., DeConto, R. M., Pollard, D., & Hu, Y. (2024). Competing climate feedbacks of ice sheet freshwater discharge in a warming world. *Nature Communications*, *15*(1), 5178. https://doi.org/10.1038/s41467-024-49604-3

Li, Q., England, M. H., Hogg, A. M., Rintoul, S. R., & Morrison, A. K. (2023). Abyssal ocean overturning slowdown and warming driven by Antarctic meltwater. *Nature*, *615*(7954), 841–847. https://doi.org/10.1038/s41586-023-05762-w

Mathiot, P., Jenkins, A., Harris, C., & Madec, G. (2017). Explicit representation and parametrised impacts of under ice shelf seas in the Z coordinate ocean model NEMO 3.6. *Geoscientific Model Development*, *10*(7), 2849–2874. https://doi.org/10.5194/gmd-10-2849-2017

Moorman, R., Morrison, A. K., & McC. Hogg, A. (2020). Thermal responses to Antarctic ice shelf melt in an eddy-rich global ocean–sea ice model. *Journal of Climate*, *33*(15), 6599–6620. https://doi.org/10.1175/JCLI-D-19-0846.1

Muilwijk, M., Hattermann, T., Beadling, R. L., Swart, N. C., Nummelin, A., Guo, C., et al. (2026). Large regional differences in antarctic ice shelf mass loss from Southern Ocean warming and meltwater feedbacks. *The Cryosphere*, *20*(2), 1087–1117. https://doi.org/10.5194/tc-20-1087-2026

Nicola, L., Notz, D., & Winkelmann, R. (2023). Revisiting temperature sensitivity: How does Antarctic precipitation change with temperature? *The Cryosphere*, *17*(7), 2563–2583. https://doi.org/10.5194/tc-17-2563-2023

Nowicki, S. M. J., Payne, A., Larour, E., Seroussi, H., Goelzer, H., Lipscomb, W., et al. (2016). Ice sheet model intercomparison project (ISMIP6) contribution to CMIP6. *Geoscientific Model Development*, *9*(12), 4521–4545. https://doi.org/10.5194/gmd-9-4521-2016

Ong, E. Q. Y., England, M. H., Doddridge, E., & Constantinou, N. C. (2025). Transient Antarctic slope current response to climate change including meltwater. *Geophysical Research Letters*, *52*(10), e2024GL113983. https://doi.org/10.1029/2024GL113983

Otosaka, I. N., Shepherd, A., Ivins, E. R., Schlegel, N.-J., Amory, C., Van den Broeke, M. R., et al. (2023). Mass balance of the Greenland and Antarctic ice sheets from 1992 to 2020. *Earth System Science Data*, *15*(4), 1597–1616. https://doi.org/10.5194/essd-15-1597-2023

Park, W., & Latif, M. (2019). Ensemble global warming simulations with idealized antarctic meltwater input. *Climate Dynamics*, *52*(5–6), 3223–3239. https://doi.org/10.1007/s00382-018-4319-8

Pauling, A. G., Bitz, C. M., Smith, I. J., & Langhorne, P. J. (2016). The response of the Southern Ocean and Antarctic sea ice to freshwater from ice shelves in an Earth System model. *Journal of Climate*, *29*(5), 1655–1672. https://doi.org/10.1175/JCLI-D-15-0501.1

Reese, R., Albrecht, T., Mengel, M., Asay-Davis, X., & Winkelmann, R. (2018). Antarctic sub-shelf melt rates via PICO. *The Cryosphere*, *12*(6), 1969–1985. https://doi.org/10.5194/tc-12-1969-2018

Reese, R., Garbe, J., Hill, E. A., Urruty, B., Naughten, K. A., Gagliardini, O., et al. (2023). The stability of present-day Antarctic grounding lines – Part 2: Onset of irreversible retreat of Amundsen Sea glaciers under current climate on Centennial timescales cannot be excluded. *The Cryosphere*, *17*(9), 3761–3783. https://doi.org/10.5194/tc-17-3761-2023

Rintoul, S. R. (2018). The global influence of localized dynamics in the Southern Ocean. *Nature*, *558*(7709), 209–218. https://doi.org/10.1038/s41586-018-0182-3

Sadai, S., Condron, A., DeConto, R., & Pollard, D. (2020). Future climate response to antarctic ice sheet melt caused by anthropogenic warming. *Science Advances*, *6*(39), eaaz1169. https://doi.org/10.1126/sciadv.aaz1169

Schmidt, G. A., Romanou, A., Roach, L. A., Mankoff, K. D., Li, Q., Rye, C. D., et al. (2023). Anomalous meltwater from ice sheets and ice shelves is a historical forcing. *Geophysical Research Letters*, *50*(24), e2023GL106530. https://doi.org/10.1029/2023GL106530

Schmidtko, S., Heywood, K. J., Thompson, A. F., & Aoki, S. (2014). Multidecadal warming of antarctic waters. *Science*, *346*(6214), 1227–1231. https://doi.org/10.1126/science.1256117

Schoof, C. (2007). Ice sheet grounding line dynamics: Steady states, stability, and hysteresis. *Journal of Geophysical Research*, *112*(F3), F03S28. https://doi.org/10.1029/2006JF000664

Seroussi, H., Nowicki, S., Payne, A. J., Goelzer, H., Lipscomb, W. H., Abe-Ouchi, A., et al. (2020). ISMIP6 Antarctica: A multi-model ensemble of the Antarctic ice sheet evolution over the 21st century. *The Cryosphere*, *14*(9), 3033–3070. https://doi.org/10.5194/tc-14-3033-2020

Siahaan, A., Smith, R. S., Holland, P. R., Jenkins, A., Gregory, J. M., Lee, V., et al. (2022). The Antarctic contribution to 21st-century sea-level rise predicted by the UK Earth System model with an interactive ice sheet. *The Cryosphere*, *16*(10), 4053–4086. https://doi.org/10.5194/tc-16-4053-2022

Silvano, A., Rintoul, S. R., Peña-Molino, B., Hobbs, W. R., van Wijk, E., Aoki, S., et al. (2018). Freshening by glacial meltwater enhances melting of ice shelves and reduces formation of antarctic Bottom Water. *Science Advances*, *4*(4), eaap9467. https://doi.org/10.1126/sciadv.aap9467

Song, P., Scholz, P., Knorr, G., Sidorenko, D., Timmermann, R., & Lohmann, G. (2025). Regional conditions determine thresholds of accelerated Antarctic basal melt in climate projection. *Nature Climate Change*, *15*(5), 1–7. https://doi.org/10.1038/s41558-025-02306-0

Stouffer, R. J., Seidov, D., & Haupt, B. J. (2007). Climate response to external sources of freshwater: North Atlantic versus the Southern Ocean. *Journal of Climate*, *20*(3), 436–448. https://doi.org/10.1175/JCLI4015.1

Swingedouw, D., Fichefet, T., Huybrechts, P., Goosse, H., Driesschaert, E., & Loutre, M.-F. (2008). Antarctic ice-sheet melting provides negative feedbacks on future climate warming. *Geophysical Research Letters*, *35*(17), L17705. https://doi.org/10.1029/2008GL034410

Tewari, K., Mishra, S. K., Dewan, A., Dogra, G., & Ozawa, H. (2021). Influence of the height of Antarctic ice sheet on its climate. *Polar Science*, *28*, 100642. https://doi.org/10.1016/j.polar.2021.100642

The IMBIE team. (2018). Mass balance of the Antarctic ice sheet from 1992 to 2017. *Nature*, *558*(7709), 219–222. https://doi.org/10.1038/s41586-018-0179-y

Thomas, M., Ridley, J. K., Smith, I. J., Stevens, D. P., Holland, P. R., & Mackie, S. (2023). Future response of Antarctic Continental shelf temperatures to ice shelf basal melting and calving. *Geophysical Research Letters*, *50*(18), e2022GL102101. https://doi.org/10.1029/2022GL102101

Willeit, M., Ganopolski, A., Kaufhold, C., Dalmonech, D., Liu, B., & Ilyina, T. (2025). Earth system response to heinrich events explained by a bipolar convection seesaw. *Nature Geoscience*, *18*(11), 1–8. https://doi.org/10.1038/s41561-025-01814-0

Winkelmann, R., Martin, M. A., Haseloff, M., Albrecht, T., Bueler, E., Khroulev, C., & Levermann, A. (2011). The potsdam parallel ice sheet model (PISM-PIK)–Part I: Model description. *The Cryosphere*, *5*(3), 715–726. https://doi.org/10.5194/tc-5-715-2011

References From the Supporting Information

Adusumilli, S., Fricker, H. A., Medley, B., Padman, L., & Siegfried, M. R. (2020). Interannual variations in meltwater input to the Southern Ocean from Antarctic ice shelves. *Nature Geoscience*, *13*(9), 616–620. https://doi.org/10.1038/s41561-020-0616-z

Albrecht, T., Martin, M., Haseloff, M., Winkelmann, R., & Levermann, A. (2011). Parameterization for subgrid-scale motion of ice-shelf calving fronts. *The Cryosphere*, *5*(1), 35–44. https://doi.org/10.5194/tc-5-35-2011

Albrecht, T., Winkelmann, R., & Levermann, A. (2020). Glacial-cycle simulations of the antarctic ice sheet with the parallel ice sheet model (PISM) – Part 1: Boundary conditions and climatic forcing. *The Cryosphere*, *14*(2), 599–632. https://doi.org/10.5194/tc-14-599-2020

Aschwanden, A., Bueler, E., Khroulev, C., & Blatter, H. (2012). An enthalpy formulation for glaciers and ice sheets. *Journal of Glaciology*, *58*(209), 441–457. https://doi.org/10.3189/2012JoG11J088

Bueler, E., Brown, J., & Lingle, C. (2007). Exact solutions to the thermomechanically coupled shallow-ice approximation: Effective tools for verification. *Journal of Glaciology*, *53*(182), 499–516. https://doi.org/10.3189/002214307783258396

Dee, D. P., Uppala, S. M., Simmons, A. J., Berrisford, P., Poli, P., Kobayashi, S., et al. (2011). The ERA-interim reanalysis: Configuration and performance of the data assimilation system. *Quarterly Journal of the Royal Meteorological Society*, *137*(656), 553–597. https://doi.org/10.1002/qj.828

Depoorter, M. A., Bamber, J. L., Griggs, J. A., Lenaerts, J. T. M., Ligtenberg, S. R. M., Van den Broeke, M. R., & Moholdt, G. (2013). Calving fluxes and basal melt rates of antarctic ice shelves. *Nature*, *502*(7469), 89–92. https://doi.org/10.1038/nature12567

Drüke, M., von Bloh, W., Petri, S., Sakschewski, B., Schaphoff, S., Forkel, M., et al. (2021). CM2Mc-LPJmL v1.0: Biophysical coupling of a process-based dynamic vegetation model with managed land to a general circulation model. *Geoscientific Model Development*, *14*(6), 4117–4141. https://doi.org/10.5194/gmd-14-4117-2021

Fretwell, P., Pritchard, H. D., Vaughan, D. G., Bamber, J. L., Barrand, N. E., Bell, R., et al. (2013). Bedmap2: Improved ice bed, surface and thickness datasets for Antarctica. *The Cryosphere*, *7*(1), 375–393. https://doi.org/10.5194/tc-7-375-2013

Garbe, J., Albrecht, T., Levermann, A., Donges, J. F., & Winkelmann, R. (2020). The hysteresis of the Antarctic ice sheet. *Nature*, *585*(7826), 538–544. https://doi.org/10.1038/s41586-020-2727-5

Gnanadesikan, A., Speller, C. M., Ringlein, G., Soucie, J. S., Thomas, J., & Pradal, M.-A. (2020). Feedbacks driving interdecadal variability in Southern Ocean convection in climate models: A coupled oscillator mechanism. *Journal of Physical Oceanography*, *50*(8), 2227–2249. https://doi.org/10.1175/JPO-D-20-0037.1

Kaufman, Z. S., Feldl, N., Weijer, W., & Veneziani, M. (2020). Causal interactions between Southern Ocean polynyas and high-latitude atmosphere–ocean variability. *Journal of Climate*, *33*(11), 4891–4905. https://doi.org/10.1175/JCLI-D-19-0525.1

Klose, A. K., Coulon, V., Pattyn, F., & Winkelmann, R. (2024). The long-term sea-level commitment from Antarctica. *The Cryosphere*, *18*(9), 4463–4492. https://doi.org/10.5194/tc-18-4463-2024

Levermann, A., Albrecht, T., Winkelmann, R., Martin, M. A., Haseloff, M., & Joughin, I. (2012). Kinematic first-order calving law implies potential for abrupt ice-shelf retreat. *The Cryosphere*, *6*(2), 273–286. https://doi.org/10.5194/tc-6-273-2012

Levermann, A., Winkelmann, R., Albrecht, T., Goelzer, H., Golledge, N. R., Greve, R., et al. (2020). Projecting Antarctica's contribution to future sea level rise from basal ice shelf melt using linear response functions of 16 ice sheet models (LARMIP-2). *Earth System Dynamics*, *11*(1), 35–76. https://doi.org/10.5194/esd-11-35-2020

Locarnini, M., Mishonov, A., Baranova, O., Boyer, T., Zweng, M., Garcia, H., et al. (2018). World ocean atlas 2018 (Vol. *1*).

Martin, T., Park, W., & Latif, M. (2013). Multi-centennial variability controlled by Southern Ocean convection in the kiel climate model. *Climate Dynamics*, *40*(7), 2005–2022. https://doi.org/10.1007/s00382-012-1586-7

Murray, R. J. (1996). Explicit generation of orthogonal grids for ocean models. *Journal of Computational Physics*, *126*(2), 251–273. https://doi.org/10.1006/jcph.1996.0136

Rignot, E., Jacobs, S., Mouginot, J., & Scheuchl, B. (2013). Ice-shelf melting around Antarctica. *Science*, *341*(6143), 266–270. https://doi.org/10.1126/science.1235798

Seroussi, H., Nowicki, S., Simon, E., Abe-Ouchi, A., Albrecht, T., Brondex, J., et al. (2019). initMIP-Antarctica: An ice sheet model initialization experiment of ISMIP6. *The Cryosphere*, *13*(5), 1441–1471. https://doi.org/10.5194/tc-13-1441-2019

van Wessem, J. M., Van de Berg, W. J., Noël, B. P. Y., Van Meijgaard, E., Amory, C., Birnbaum, G., et al. (2018). Modelling the climate and surface mass balance of polar ice sheets using RACMO2–Part II: Antarctica (1979–2016). *The Cryosphere*, *12*(4), 1479–1498. https://doi.org/10.5194/tc-12-1479-2018

Zhang, L., Delworth, T. L., Cooke, W., Goosse, H., Bushuk, M., Morioka, Y., & Yang, X. (2021). The dependence of internal multidecadal variability in the Southern Ocean on the ocean background mean state. *Journal of Climate*, *34*(3), 1061–1080. https://doi.org/10.1175/JCLI-D-20-0049.1

Zweng, M., Reagan, J., Seidov, D., Boyer, T., Locarnini, M., Garcia, H., et al. (2019). World ocean atlas 2018. *Salinity (Report)*, *2*.